International Journal of Physical Sciences

Academic Journals

ABOUT IJPS

The **International Journal of Physical Sciences (IJPS)** is published weekly (one volume per year) by Academic Journals.

International Journal of Physical Sciences (IJPS) is an open access journal that publishes high-quality solicited and unsolicited articles, in English, in all Physics and chemistry including artificial intelligence, neural processing, nuclear and particle physics, geophysics, physics in medicine and biology, plasma physics, semiconductor science and technology, wireless and optical communications, materials science, energy and fuels, environmental science and technology, combinatorial chemistry, natural products, molecular therapeutics, geochemistry, cement and concrete research, metallurgy, crystallography and computer-aided materials design. All articles published in IJPS are peer-reviewed.

Contact Us

International Journal of Physical Sciences

ARTICLES

Full Length Research Paper

Primordial radionuclides in potable water from former tin-mining areas with elevated activity

O. I. Adekoya[1,2]

[1]Physics Department, University of Ibadan, Oyo, Nigeria.
[2]Physical Science Department, Yaba College of Technology, Lagos, Nigeria.

The activity concentrations of the primordial radionuclides in potable water from 2 former mining areas (Bisichi and Bukuru) in Jos, Plateau state in Nigeria have been studied. The activities were determined by a non-destructive analysis using a computerized gamma ray spectrometry system with high purity germanium (HPGe). The results show the average activity concentrations for ^{226}Ra, ^{232}Th and ^{40}K for Bukuru and Bisichi to be respectively 1.20 ±0.02, 1.93 ± 0.01, 4.75 ± 0.14 and 2.03 ± 0.14, 2.20 ± 0.13 and 3.26 ± 0.06 Bq/l. The corresponding annual effective doses for both locations are respectively 0.59 and 0.80 mSv/year which are much higher than the reference level of a dose of 0.1mSv/year from the intake of drinking water.

Key words: Activity concentration, radionuclides, drinking water.

INTRODUCTION

Environmental radiation originates from a number of naturally occurring and man-made sources. The United Nations Scientific Committee on the Effects of Atomic Radiation (UNSCEAR) has estimated that exposure to natural sources contributes more than 98% of the radiation dose to the population (excluding medical exposure) (UNSCEAR, 1998)

The global average human exposure from natural sources is 2.4 mSv/year (UNSCEAR 1993). There are however, large local variations in this exposure depending on a number of factors, such as height above sea level, the amount and type of radionuclides in the soil, and the amount taken into the body in air, food and water.

Research reports on environmental radioactivity studies

in the Jos Plateau have indicated high gamma radiation dose rates several orders of magnitude higher than world average value (Oresegun and Babalola, 1990, 1993; Farai and Jibiri, 2000). Majority of these reports attributed these high levels primarily on the influence of tin and its mining activities in the area (Farai and Jibiri, 2000; Jibiri et al., 2007a, b; Ademola, 2008).

The negative impact of tin mining activities such as occurred in Bukuru and Bisichi areas in Jos, Plateau, Nigeria, on the environment is mainly due to the excavation of large amounts of sand and the eventual accumulation of a large volume of tailings (Banat et al., 2005; Remon et al., 2005; Akinlua et al., 2006; Birkefeld et al., 2006; Nyarko et al., 2006), which significantly alter the natural constituents of radionuclides in the soil and
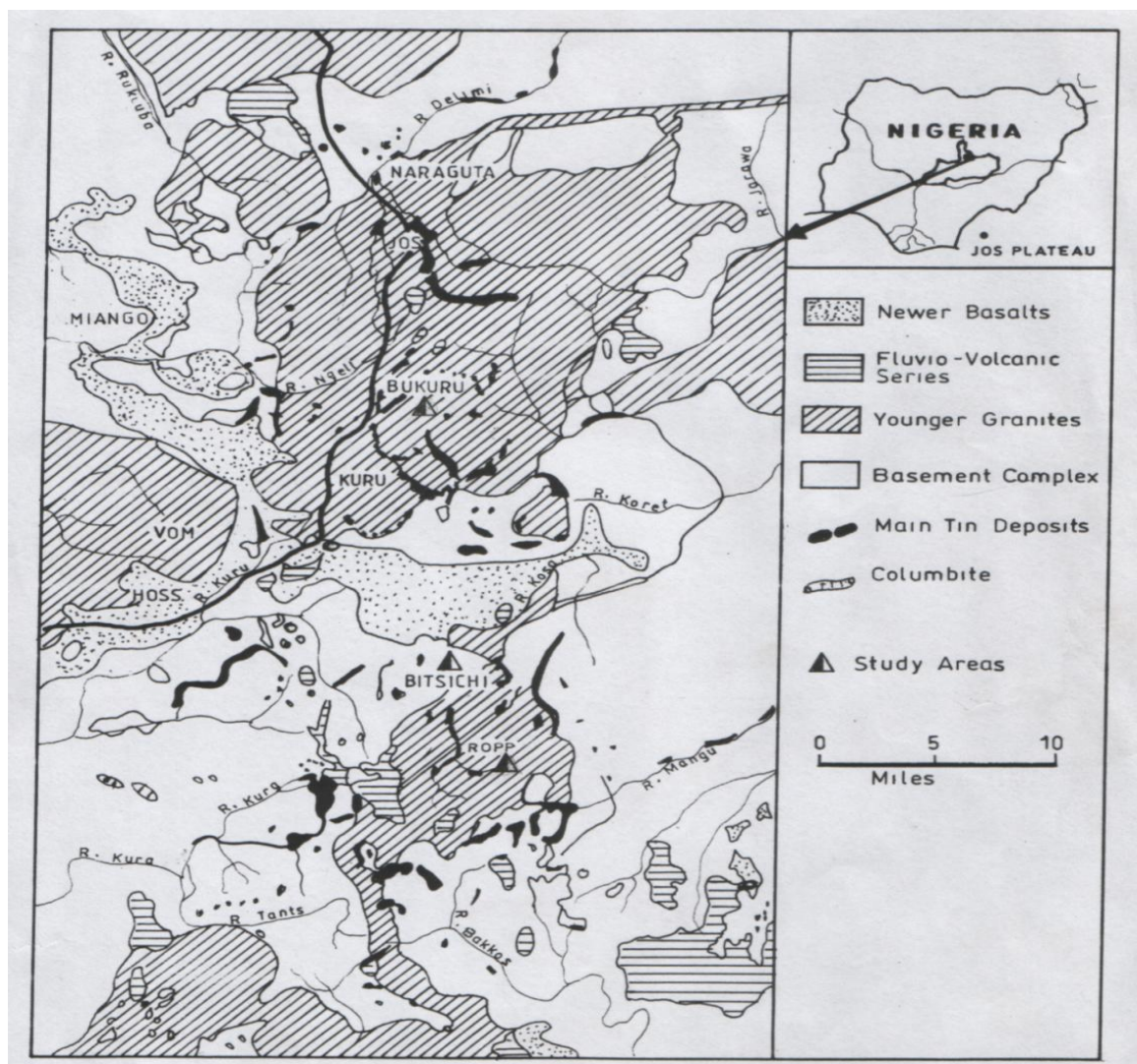
Figure 1. The map of Jos Plateau showing the study locations (Jibiri et al., 2011).

thus affect the terrestrial ecosystem.

Indiscriminate and improper deposition of tailings, especially on steep slopes, increases their mobility and hence the risk of being transported to large inhabited areas (Henriques and Fernandes, 1991). Due to leaching and re-suspension processes, ^{238}U and ^{232}Th from abandoned dumping sites find their way in surface and ground water (Ragnarsdottir and Charlet, 2000). Consequently, this makes mine tailings a source of pollution to the ground and surface water, and to the soil in their vicinities (Hector et al., 2006).

The process of leaching as well as washing away of tailings due to erosion activities into surface and ground water is what goes on at Bukuru and Bisichi areas of Jos, Plateau in Nigeria. The tailings may accumulate to extents that could be detrimental to human lives, where this water is either drunk directly or used in processing foods.

The present research focuses on the assessment of radioactivity in potable water from dams and wells in Bukuru and Bisichi areas of Jos, Plateau, as well as the effective doses to the dwellers in these areas.

MATERIALS AND METHODS

Sample collection and preparation

Drinking water samples were collected from dams and wells from two former tin-mining locations –Bukuru and Bisichi, in Jos, Plateau state, Nigeria. Other water bodies in these areas were discarded once it was established that they were not sources of drinking water. The map of the locations in question is shown in Figure 1.

The bottles were filled to the brim without any head space to prevent trapping of radon gas. For activity concentration measurement, the water samples were also transported to the laboratory and prepared into 1 L Marinelli beakers. The samples were filtered prior to preparation and measurements.   The beakers

Table 1. Activity concentration of water samples.

S/No	Description	^{226}Ra(Bq/l)	^{232}Th(Bq/l)	^{40}K(Bq/l)
1	BS-Dam	1.66 ± 0.23	2.00 ± 0.30	0.25 ± 0.01
2	BS-Well water 1	2.11 ± 0.08	3.14 ± 0.05	9.33 ± 0.16
3	BS-Well water 2	2.33 ± 0.10	1.46 ± 0.04	0.20 ± 0.01
4	BK Dam1	<MDL	0.17 ± 0.01	0.16 ± 0.01
5	BK Dam 2	1.62 ± 0.04	3.08 ± 0.02	5.38 ± 0.22
6	BK Dam 3	3.17 ± 0.02	2.77 ± 0.01	13.24 ± 0.32
7	BK Dam 4	<MDL	1.70 ± 0.01	0.20 ± 0.01

BS, Bitsichi; BK, Bukuru, MDL, minimum detection limit.

were thick enough to prevent the permeation of radon. The beakers were closed by screw caps and plastic tape was wrapped over the caps and then stored for measurement. This step was necessary to ensure that radon gas is confined within the volume and that the daughters will also remain in the sample. The samples were sealed for thirty days in order to allow for Radon and its short-lived progenies to reach secular radioactive equilibrium prior to gamma spectroscopy.

Sample measurement and analysis of spectra

All measurements were carried out at the Ghana Atomic Energy Commission, Accra. The activity concentrations of the water samples were determined by a non-destructive analysis using a computerized gamma ray spectrometry system with high purity germanium (HPGe). The relative efficiency of the detector system was 25%, and resolution of 1.8 keV at 1.33 MeV of ^{60}Co. The gamma spectrometer is coupled to conventional electronics connected to a multichannel analyzer card (MCA) installed in a desk top computer. A software program called MAESTRO- 32 was used to accumulate and analyze the data manually using spread sheet (Microsoft Excel) to calculate the natural radioactivity concentrations in the samples. The detector is located inside a cylindrical lead shield of 5 cm thickness with internal diameter of 24 cm and height of 60 cm. The lead shield is lined with various layers of copper, cadmium and Plexiglas, each 3 mm thick.

A counting time of 36,000 s (10 h) was used to acquire spectral data for each sample. The activity concentrations of the uranium-series were determined using γ-ray emissions of ^{214}Pb at 351.9 keV (35.8%) and ^{214}Bi at 609.3 keV (44.8%) for ^{226}Ra, and for the ^{232}Th-series, the emissions of ^{228}Ac at 911 keV (26.6%), ^{212}Pb at 238.6 keV (43.3%) and ^{208}Tl at 583 keV (30.1%) were used. The ^{40}K activity concentration was determined directly from its emission line at 1460.8 keV (10.7%).

Calibration of gamma spectrometry system

Prior to the measurements, the detector and measuring assembly were calibrated for energy and efficiency to enable both qualitative and quantitative analysis of the samples to be performed. The energy and efficiency calibrations were performed using mixed radionuclide calibration standard homogenously distributed in the form of solid water, serial number NW 146 with approximate volume 1000 ml and density 1.0 g cm^{-3} in a 1.0 L Marinelli beaker. The standard was supplied by DeutscherKalibrierdienst (DKD-3), QSA Global GmBH, Germany and contains radionuclides with known energies (^{241}Am (59.54 keV), ^{109}Cd (88.03 keV), ^{57}Co (122.06 keV), ^{139}Ce (165.86 keV), ^{203}Hg (279.20 keV), ^{113}Sn (391.69 keV), ^{85}Sr

(514.01 keV), ^{137}Cs (661.66 keV), ^{60}Co (1173.2 keV and 1332.5 keV) and ^{88}Y (898.04 keV and 1836.1 keV) and activities in a 1000 ml Marinelli beaker was used.

Calculation of activity concentration

The specific activity concentrations (A$_{sp}$) of ^{226}Ra, ^{232}Th, ^{40}K in Bq l^{-1} for the water were determined using the following expression (Beck et al., 1972):

$$A_{sp} = \frac{N_{sam}}{P_E.\varepsilon.T_c.M} \tag{1}$$

Where; N_{sam} = net counts of the radionuclide in the sample; P_E = gamma ray emission probability (gamma yield); ε = total counting efficiency of the detector system; T_c = sample counting time; M = mass of sample (kg) or volume (L)

Minimum detectable activity

The minimum detectable activity (MDA) of the γ-ray measurements were calculated according to the formula:

$$MDA = \frac{\sigma\sqrt{B}}{\varepsilon PTW} \text{ (Bqkg}^{-1}) \tag{2}$$

Where σ is the statistical coverage factor equal to 1.645 confidence level 95%, B is the background counts for the region of interest of a certain radionuclide, T is the counting time in seconds, P is the gamma yield for any particular element, W is the weight of the empty Marinelli beaker and ε is the efficiency of the detector.

The minimum detectable activity (MDA) derived from background measurements was approximately 0.11 Bq kg^{-1} for ^{226}Ra, 0.10 Bq kg^{-1} for ^{232}Th and 0.15 Bq kg^{-1} for ^{40}K. Concentration values below these detection limits have been taken in this work to be below the minimum detection limit (MDL).

RESULTS AND DISCUSSION

Primordial radionuclide activity in water

The results for the primordial radionuclide activity in the drinking water samples are shown in Table 1 and Figures 2 to 4.
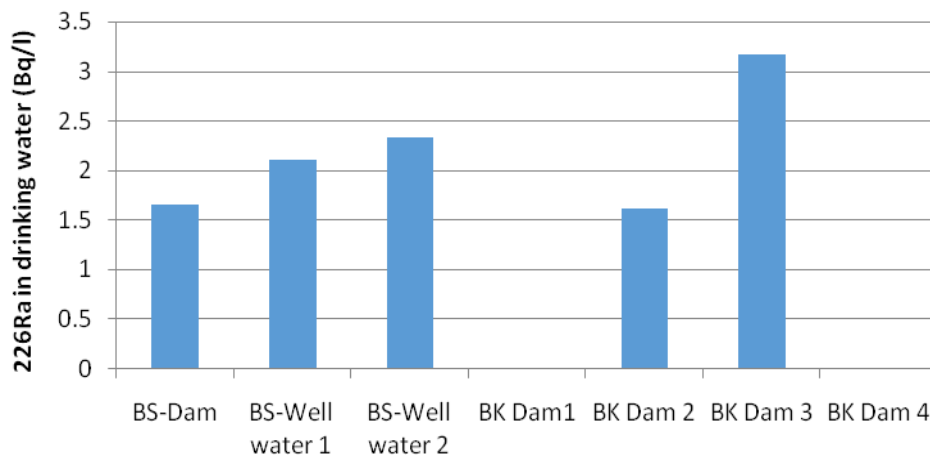
Figure 2. Activity concentration of ^{226}Ra in water samples.
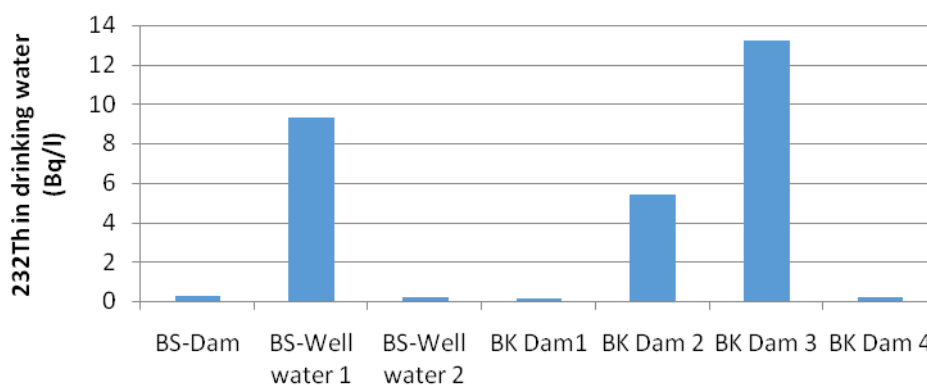

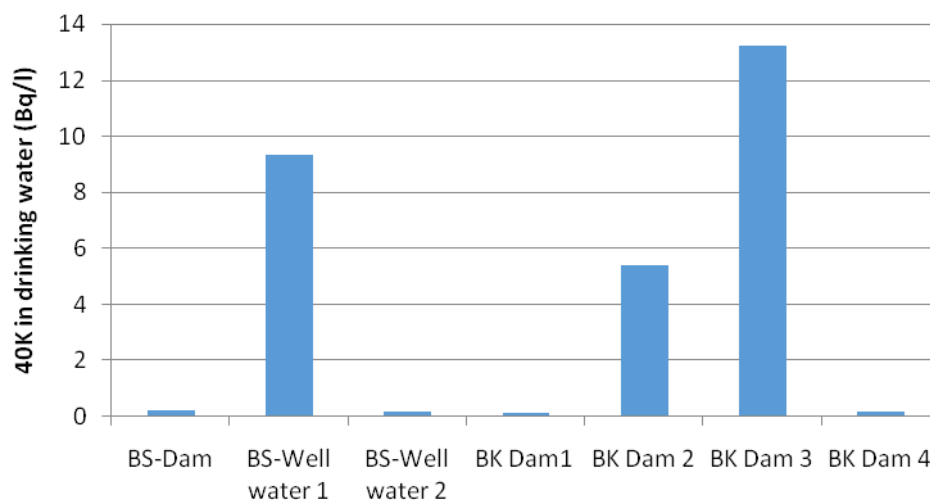**Figure 3.** Activity concentration of ^{232}Th in water samples.

Figure 4. Activity concentration of ^{40}K in water samples.

The highest activities for the radionuclides of interest were noticed in the water sample from the dam 3 in Bukuru. This could only suggest that mining activities was very much pronounced in that vicinity. The water sample

Table 2. Annual effective dose from ingested water in Bukuru and Bisichi.

Location	Average activity concentration (Bq/l)			Annual effective dose (µSv/year)			
	^{226}Ra	^{232}Th	^{40}K	^{226}Ra	^{232}Th	^{40}K	Total
Bukuru	1.20	1.93	4.75	245.3	324	21.5	590.8
Bitsichi	2.03	2.20	3.26	415	369	14.8	798.8

Table 3. Effective doses from ingested water in different European counties (Vesterbacka, 2005).

Country	Effective dose (mSv)	Radionuclides included in the dose estimation
Finland	0.39	^{222}Rn,^{226}Ra,^{238}U, ^{234}U, ^{210}Po,^{210}Pb
Sweden	0.51	^{222}Rn,^{226}Ra,^{228}Ra,^{210}Po,^{238}U
Ukraine	0.22	^{222}Rn,^{226}Ra,^{238}U
Denmark	0.16	^{222}Rn, ^{226}Ra
Switzerland	0.03	^{238}U,^{226}Ra, ^{228}Ra
Scotland	0.05	^{222}Rn
Austria	0.12	^{226}Ra
Spain	4.2	Long lived radionuclides
Hungary	<0.1	^{222}Rn,^{226}Ra
Greece	<0.05	^{222}Rn
Bukuru (this work)	0.59	^{226}Ra, ^{232}Th ,^{40}K
Bisichi (this work)	0.80	^{226}Ra, ^{232}Th ,^{40}K

from well 1 in Bitsichi showed a similar trend except that Ra-226 activity in the sample was lower compared to that in well water 2. The least activities were observed in water samples from dam 1 in Bukuru, where Ra-226 was below minimum detection limit. The average activity concentrations for ^{226}Ra, ^{232}Th and ^{40}K for Bukuru and Bisichi are respectively 1.20 ±0.02, 1.93 ± 0.01, 4.75 ± 0.14Bq/l and 2.03 ± 0.14, 2.20 ± 0.13, 3.26 ± 0.06 Bq/l.

It follows from the results that the activities of ^{226}Ra and ^{232}Th on the average are higher in Bitsichi than in Bukuru, unlike ^{40}K which shows the reverse. Furthermore, the concentration of ^{226}Ra on the average is more in well water compared to the dams. The reason for the latter is due to the fact that ground water (well water) flows through fractured rock carrying radioactive materials and other elements from the solid to the liquid phase.

The annual effective dose from radionuclide in drinking water was computed using the following equation, assuming a daily water intake of 2 L/day (EPA, 2000-2005):

$$Reference\ Concentration\,(Bq/l) = \frac{Dose\,(Sv/yr)}{730\,(litre/yr)*dose\ conversion\ factor\,(Sv/Bq)} \quad (3)$$

The dose conversion factors of 2.8×10^{-7}(Sv/Bq), 2.3×10^{-7}(Sv/Bq) and 6.2×10^{-9}(Sv/Bq) were respectively used for ^{226}Ra, ^{232}Th and ^{40}K (ICRP, 1996) (Table 2).

A comparison of the results with those for different European countries (Table 3) shows that the values obtained in this work are higher. The results obtained in this work are approximately 0.59 and 0.80 mSv/year for Bukuru and Bitsichi respectively which is much higher than the reference level of a dose of 0.1 mSv/year from the intake of potable water.

Conclusion

The activity concentrations of the primordial radionuclides in potable water from Bitsichi and Bukuru, former tin-mining areas in Jos, Plateau were investigated. The results show that internationally recommended minimum acceptable values were exceeded; the contributory factor being likely as a result of the tin- mining activities that had been carried out in the area in the past. There is need for proper water treatment in the areas in order to reduce health risks due to ingested radionuclides.

Conflict of Interest

The authors have not declared any conflict of interest.

the collection of samples from the dams in Bitsichi and Bukuru areas of Jos, Plateau state. The efforts of David Okoh and Nicholas Sackitey of the Radiation Protection Institute, Ghana Atomic Energy Commission, Accra in the measurement of the samples is also appreciated.

REFERENCES

Akinlua A, Ajayi TR, Adeleke BB (2006). Preliminary assessment of rare earth element contents of Niger-Delta oils. J. Appl. Sci. 6:11–14. http://dx.doi.org/10.3923/jas.2006.11.14

Banat KM, Howari FM, Al-Hamad AA (2005). Heavy metals in urban soils of central Jordan: should we worry about their environmental risks? Environ. Res. Section A 97:258–273. http://dx.doi.org/10.1016/j.envres.2004.07.002

Beck HL, Decompo J, Gologak J (1972). *In situ* Ge (ii) and NaI(Tl) gamma ray spectrometry, In: Otoo*et al*, 2011, Assessment of Natural Radioactive Materials used along the Coast of Central region of Ghana. Res. J. Environ. Health Sci. 3(3):261-268. http://dx.doi.org/10.2172/4599415

Birkefeld A, Schulin R, Newack B (2006). In situ investigation of dissolution of heavy metal containing mineral particles in an acidic forest soil. Geochimicaet. Cosmo. chimica. Acta. 70:2726–2736.

Farai IP, Jibiri NN (2000). Baseline studies of terrestrial outdoor gamma dose rate levels in Nigeria. Radiation Protect. Dosimetry 88:247-254. http://dx.doi.org/10.1093/oxfordjournals.rpd.a033042

Hector MC, Angel F, Raquel A (2006). Heavy metal accumulation and tolerance in plants from mine tailings of the semiarid Cartagena-La Union mining district (SE Spain). Sci. Total Environ. 366:1–11. http://dx.doi.org/10.1016/j.scitotenv.2005.12.008

Henriques FS, Fernandes JC (1991). Metal uptake and distribution in rush (Juncusconglomeratus L.) plants growing in pyrites mine tailings at Lousal, Portugal. Sci. Total Environ.102:253–260. http://dx.doi.org/10.1016/0048-9697(91)90319-A

ICRP (1996). Age-dependent Doses to the Members of the Public from Intake of Radionuclides Part5, Compilation of Ingestion and Inhalation Coefficients. International Commission of Radiological Protection Publication 72. Pergamon Press, Oxford.

Jibiri NN, Farai IP, Alausa SK (2007a). Estimation of annual effective dose due to natural radioactive elements in ingestions of foodstuffs in tin mining area of Jos-Plateau, Nigeria. J. Environ. Radioact. 94:31-40. http://dx.doi.org/10.1016/j.jenvrad.2006.12.011

Jibiri NN, Farai IP, Alausa SK (2007b). Activity concentrations of 226Ra, 228Th, and 40K, in different food crops from a high background radiation area in Bitsichi, Jos Plateau, Nigeria. Radiation Environ. Biophy. 46:53–59. http://dx.doi.org/10.1007/s00411-006-0085-9

Jibiri NN, Alausa SK, Owofolaju AE, Adeniran AA (2011). Terrestrial gamma dose rates and physical-chemical properties of farm soils from ex- tin mining locations in Jos-Plateau, Nigeria. Afr. J. Environ. Sci. Technol. 5(12):1039-1049. December 2011. http://dx.doi.org/10.5897/AJEST11.245

Nyarko BJB, Adomako D, Serfor-Armah Y, Dampare SB, Adotey D Akaho EHK (2006). Biomonitoring of atmospheric trace element deposition. Radiat. Phys. Chem. 75:954-958. http://dx.doi.org/10.1016/j.radphyschem.2005.08.021

Oresegun MO, Babalola IA (1990). Occupational radiation exposure associated with milling of Th-U rich Sn in Nigeria. Health Phy. 58:213-215.

Oresegun MO, Babalola IA (1993). The environmental gamma radiation level of Jos, Nigeria. Nig. J. Sci. 27:263–268.

Remon E, Bouchardon JL, Cornier B, Guy B, Leclerc JC, Faure O (2005). Soil characteristics, heavy metal availability and vegetation recovery at a formal metallurgical landfill: implication in risk assessment and site restoration. Environ. Pollut. 137:316–323. http://dx.doi.org/10.1016/j.envpol.2005.01.012

Ragnarsdottir KV, Charlet L (2000). Uranium behaviour in natural environments. In: Environmental Mineralogy: Microbial Interactions, Anthropogenic Influences, Contaminate Land and Waste Management. The Mineralogical Society of Great Britain & Ireland.

U.S Environmental Protection Agency (EPA). Dallas, Tx (2000 – 2005) 'Chapter 3: Exposure Scenarion Selection' (http://www.epa.gov/earth1r6/6pd/rcra_c/pd-o/chap3 pdf

UNSCEAR (1993). Sources, Effects and Risks of Ionizing Radiation. United Nations Scientific Committee on the Effects of Atomic Radiation, New York. Report to the General Assembly on the Effects of Atomic Radiation, United Nations.

UNSCEAR (1998). Sources, Effects and Risks of Ionizing Radiation. United Nations Scientific Committee on the Effects of Atomic Radiation, New York. Report to the General Assembly on the Effects of Atomic Radiation, United Nations.

Vesterbacka P (2005). U-238 series radionuclides in Finnish groundwater-based drinking water and effective doses. Academic dissertation.

Full Length Research Paper

Theoretical studies of CO converted to CH₃OH by ZINDO/1-DFT methods

Leila Mahdavian

Department of Chemistry, Doroud Branch, Islamic Azad University, P.O. Box: 133. Doroud Iran.

The aim of this study is to simulate co-catalysts of titanium nitride nanotubes (TiN-NTs) with Cu nano-particles for converting carbon monoxide (CO) and water into methanol. This method may provide a new way to reduce carbon-monoxide levels in the atmosphere rising due to our planet's heavy use of fossil fuels as well as to produce alternative fuels. Using TiN-NTs has shown the efficiency to remove CO from the atmosphere. There are four positions for CO and TiN-NTs (4, 4) that we have investigated, passing of CO endohedrally and between the nanotubes. We study the structural, total energy, thermodynamic and conductive properties of converted CO on Cu nano-particles in TiN-NTs to methanol. The electronic and geometric structures and thermodynamic properties are quantum mechanically calculated for these situations by DFT methods at the semi-empirical ZINDO/1 level, B3LYP/6-31G basis sets. The thermodynamic properties show which interactions are endothermic. The heat of exhaust can be used for CO conversion to CH₃OH or other products.

Key words: Carbon monoxide (CO), Methanol, Titanium nitride nanotubes (TiN-NTs), ZINDO/1, environment.

INTRODUCTION

Carbon monoxide (CO) is a colorless, odorless, and tasteless gas that is somewhat less dense than air. It is dangerous to humans and animals when withstood in larger levels, though it is also produced in standard pet metabolism in minimal amounts, and is considered to have some standard organic functions. In the air, it is spatially variable and temporary, having a role in the formation of ground-level ozone (Riduan et al., 2009).

Solid state gas sensors are most important in semiconductor processing, medical diagnosis, environmental sensing, and personal safety etc. (Kolmakov et al., 2003). The high surface to volume ratio of nano-forms makes them natural contenders as new sensors and suitable surface to remove and converted pollutants.

TiN-nanotubes (TiN-NTs) have attracted great interest due to their unique electronic properties and nanometer size. Because of these unique properties, they are great potential candidates in many important applications such as nanoscale electronic devices, chemical sensors and field emitters. The effect of gas adsorption on the electrical resistance of a TiN-NT has received great attraction because of fast response, good sensitivity of chemical environment gases and low operating temperature (Paulose et al., 2006).

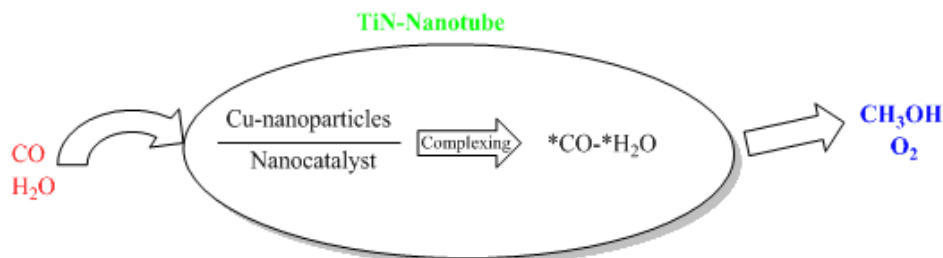The products of the carbon monoxide (CO) and water

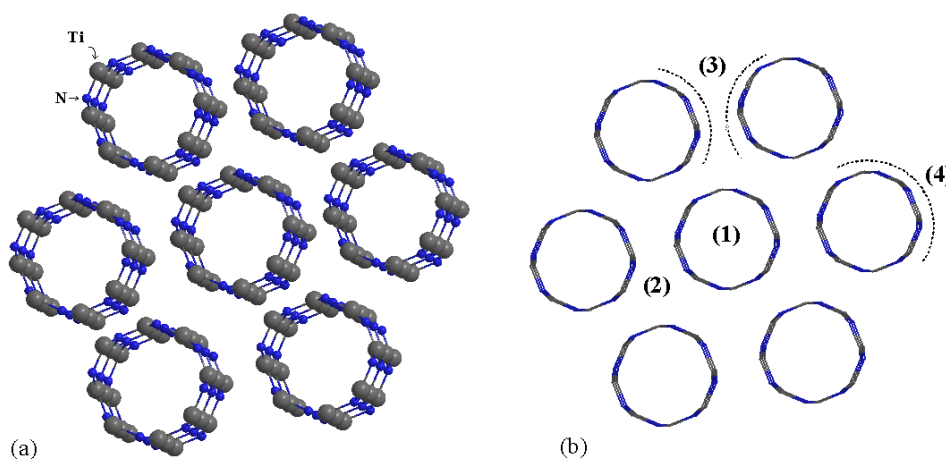**Figure 1.** The conversion of CO into methanol.

Figure 2. There are four situations for interaction CO and H_2O in TiN-nanotube, (a) Ball-and-stick and (b) stick models Configuration for them.

(H_2O) reaction depend on metal oxide catalysis, temperature and pressures [Li et al., 2007]. The most important challenge is that of the catalyst. The current commercial catalysts are co-catalysts of titanium nitride nanotubes with Cu- nanoparticles that help converts carbon monoxide and water into methanol using sunlight as the power source for sun gas conversion (Figure 1). There are some methods such as options for carbon monoxide and carbon dioxide removal from the atmosphere include afforestation and chemical approaches like direct air capture of CO from the atmosphere or reactions of CO with minerals to form carbonates [Varghese et al., 2009; Farha et al., 2010; Yang et al., 2012; Aresta and Dibenedetto, 2004; Hohenberg and Kohn, 1964]. Methane and methanol are major products of the chemical industry and also a feedstock for many chemicals. However CO conversion to methanol and other product is challenging.

As shown in Figure 2, there are four situations in which CO and H_2O can pass between TiNNTs-Cu. In this work, the 1st and 2nd situations are investigated for them. In Figures 3 and 4, TiN- nanotubes with Cu-nanoparticle simulated by ball-and-stick models, CO and H_2O converted to CH_3OH and O_2.

Interaction between CO and H_2O on Cu nanoparticle in TiN-nanotubes is investigated using ZINDO/1 method by semi empirical. We study the structural, total energy, thermodynamic properties of them in room temperature. All the geometry optimization structures were carried out using Gaussian program package. Density Functional Theory (DFT) optimized their intermediates and transient states. The results show a sensitivity enhancement in resistance and capacitance when CO and H_2O are converted to CH_3OH and O_2.

THE COMPUTATIONAL METHODS

The computational approach consists of three stages: First, all the geometry optimization structures in present work were performed by employing DFT, using Becke's three parameter hybrid with the Lee-Yang-Parr correlation functional, B3LYP (Becke, 1993; Yang and Parr, 1988) method with the 6-31G basis sets. Then the thermodynamic properties of them were calculated for different distances. We can use the information obtained from semi-empirical calculations to investigate many thermodynamic aspects of chemical processes. The heat of formation is calculated by subtracting atomic heats of formation from the binding energy. ZINDO/1 has been used widely to calculate heats of formation, molecular geometries, dipole moments, ionization energies,
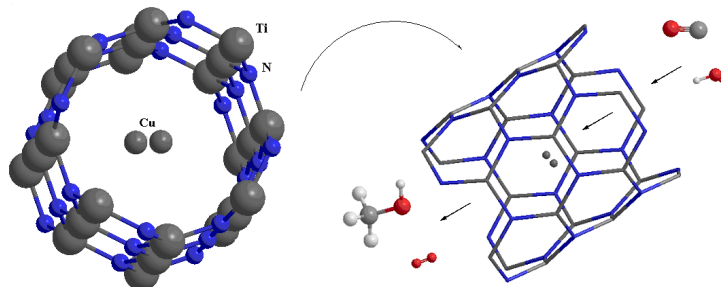
Figure 3. Ball-and-stick models configuration: Top-view of first situation passing CO and H_2O endohedral of TiN-nanotube with Cu-nanoparticle.
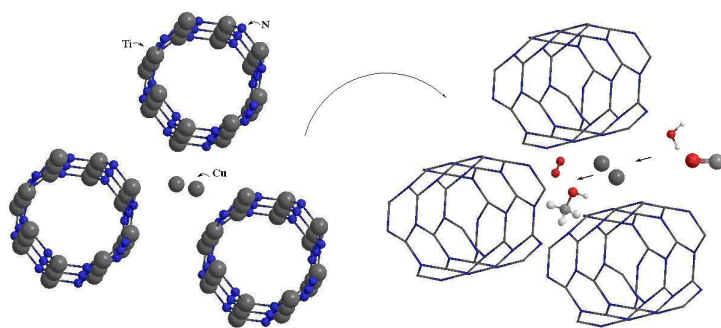

Figure 4. Ball-and-stick models configuration: Top-view of second situation passing CO and H_2O between TiN-nanotube with Cu-nanoparticle.

RESULTS AND DISCUSSION

The electronic structures and properties of CO converted to CH_3OH have been investigated using hybrid density functional theories with the basis set B3LYP/6–31G use correct logical order. In this work, we use TiN-NTs from kind of armchair TiN nanotubes (4, 4) that show in Figures 3 and 4. When CO gas from the exhaust exits to the filter of TiN-NTs with Cu nanoparticles (into or between of TiN-NTs), electron exchange between them occurs and CO converts to CH_3OH or other products. Table 1 show thermodynamice parameters of monoxide carbon and water endohedral passing in TiN-NT by

electron affinities, and other properties (Ridley and Zerner, 1973; Zerner, 1991). At the end, the reaction pathway is analyzed in order to confirm the structure of the transition state obtained.

In this study, entry carbon monoxide and water on Cu nanoparticles between titanium nitride nanotubes have been simulated in three steps (Figures 3 and 4), and then in steps 4 and 5 are transition state conversion of them to CH_3OH and O_2. The conversion was completed in 6th step, methanol and oxygen are produced, and then it is excretion from TiN-NTs in 7th or 8th step. The electronic structure and the thermodynamic properties are calculated for all steps by ZINDO/1.

seven steps and their passing between TiN-nanotubes (second state) shown in Table 2. The thermodynamic properties for all steps are without the effect of the catalyst in the reaction for example:

$$\Delta E_{total} = E_{(TiN\text{-}Cu + CO+ water)} - E_{(TiN\text{-}Cu)} \qquad (1)$$

The study includes conformational searches (and further refinement by DFT) and semi- empirical by ZINDO/1 methods. The most significant property is the ZINDO/1, which is, finding a good correlation between the ZINDO/1 and the substitution pattern on this conversation. ZINDO/1 has been used widely to calculate heats of formation, molecular geometries, dipole moments, ionization energies, electron affinities, and other properties (Reslan et al., 2012; Dondela et al., 2005).

In Tables 1 and 2, the dipole moment (D) measurement gives an idea about the degree of polarity for approached of CO and H_2O to Cu nanoparticles into and between TiN-NT. When CO passing in nanotube, dipole moment (D) decrease, so in 4th and 5th steps increase polar because in these steps occur exchange electron between them and is formed CH_3OH and O_2 for two situations. The root mean square (RMS) gradient (kcal/mol. Å) is different for this interaction at room temperature.

Table 1. The thermodynamic properties of interaction CO and H_2O into Cu-TiN nanotube (4, 4) to CH_3OH at 298K (ZNDO/1).

	The CO and H_2O endohedral passing in Cu-TiN nanotube						
	E_{total} (kJ/mol)	E_{nuc} (kJ/mol)	Dipol Moment (D)	RMS kcal/mol.^{o}A	E_{bin} (kJ/mol)	H (kJ/mol)	G_{elec} (kJ/mol)
TiN-Cu	1845450	8280830	3012	1.63×10^4	2984390	3007790	3064840
Steps	ΔE_{total} (kJ/mol)	ΔE_{nuc} (kJ/mol)	Δ(Dipol Moment) (D)	Δ(RMS) kcal/mol.^{o}A	ΔE_{bin} (kJ/mol)	ΔH (kJ/mol)	ΔG_{elec} (kJ/mol)
1	234770	1021660	25	-0.06×10^4	34010	341740	374420
2	462610	1163420	10	-0.08×10^4	56794	569580	333890
3	330140	1351290	4	-0.07×10^4	43547	437100	486360
4	51650	1604210	247	-0.12×10^4	15698	158620	739190
5	582100	2020920	337	-0.13×10^4	73393	736260	685150
6	588500	1910460	22	-0.09×10^4	74033	742660	629180
7	404040	1632390	69	-0.09×10^4	55584	558170	584790

Table 2. The thermodynamic properties of interaction CO and H_2O between Cu-TiN nanotube (4,4) to CH_3OH at 298K (ZNDO/1).

	The CO and H_2O passing between Cu-TiN nanotube						
	E_{total} (kJ/mol)	E_{nuc} (kJ/mol)	Dipol Moment (D)	RMS kcal/mol.^{o}A	E_{bin} (kJ/mol)	H (kJ/mol)	G_{elec} (kJ/mol)
3TiN-Cu	18844550	39060150	1741	8335	21706320	2177513	962877
Steps	ΔE_{total} (kJ/mol)	ΔE_{nuc} (kJ/mol)	Δ(Dipol Moment) (D)	Δ(RMS) kcal/mol.^{o}A	ΔE_{bin} (kJ/mol)	ΔH (kJ/mol)	ΔG_{elec} (kJ/mol)
1	-4033420	1210270	328	2125	-3928100	-3926440	2497420
2	-3017480	1560550	214	1461	-5879250	-2910500	2180900
3	2203560	1654000	24	122	2308870	2310530	-262480
4	-4737300	1778780	435	2345	-4631990	-4630340	3103440
5	-3521920	1960840	422	2565	-3416610	-3414950	2611290
6	2488480	2776170	20	-94	2640300	2642640	137030
7	3152810	2448490	58	181	3304630	3306970	-335820
8	1828020	1608430	66	-149	1979840	1982190	-106150

The total energy (E_{total}) is minimum amount for 4th step, is 51650 (endohedral) and -4737300 kJ/mol (between tube), after its conversion, E_{total} increase to 582100 kJ/mol in 5th step for endohedral passing and -3521920 kJ/mol for between passing (Figures 5 and 6).

The ΔE_{nuc}, ΔE_{bin}, ΔH and ΔG_{elec} increase in 5th step that methanol molecule is formed in this interaction for tow situations. Thermodynamic equilibrium constants, K, for these interactions were calculated by the related standard Gibbs free energy difference (ΔG_{elec}):

$$K = \exp\ (-\Delta G_{elec}/RT\ ) \qquad (2)$$

Where, T is the transition temperature and R is gas constant. The entropy difference (ΔS) at the phase transitions are given by:

$$\Delta S = \frac{\Delta H}{T} \qquad (3)$$

Where, ΔH is the electronic enthalpy difference. In Table 3 is shown the other thermodynamic properties for these interactions.

Thermodynamic parameters (ΔG_{ele}, ΔH_{ele} and ΔS_{ele}) for CO and H_2O converted to CH_3OH and O_2 were calculated and the results suggest that the nature of adsorption is endothermic.

This method needs energy that can be provided from heat of exhaust gas or solar energy. The calculation of thermodynamics is evaluated due to the comparison with experimental values. The calculated data are in good agreement with the experimental spectra (Varghese et al., 2009).

Conversion of CO by TiN-nanotube is caused changing in the electric structure of nanotube, because CO and
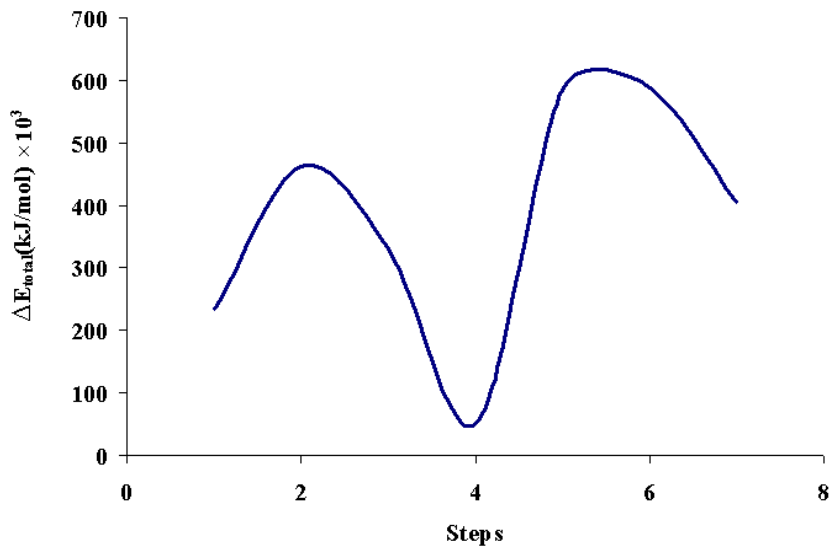
Figure 5. The total energy (MJ/mol) of converted CO and H_2O to CH_3OH into Cu-TiN nanotube.
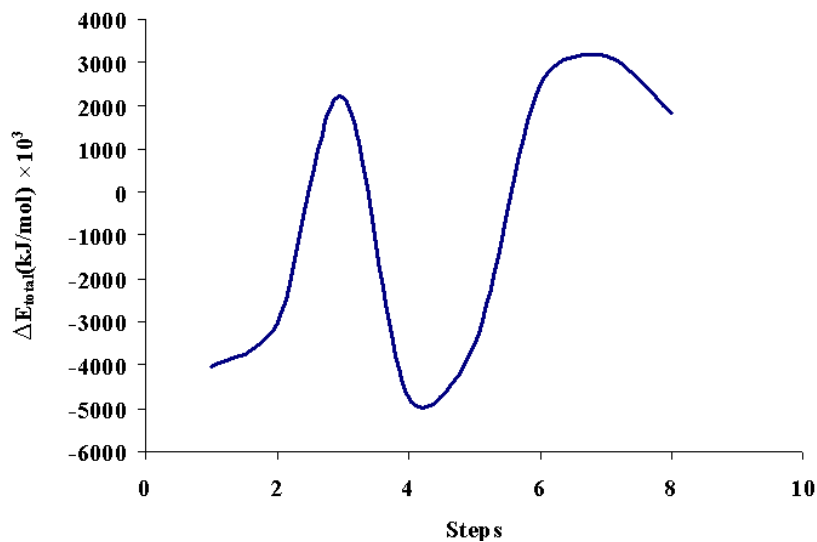
Figure 6. The total energy (kJ/mol) of converted CO and H_2O to CH_3OH between Cu-TiN nanotubes.

Table 3. The thermodynamic properties of CO and H_2O passing Cu-TiN and convert to CH_3OH and O_2.

	ΔG_{ele} (kJ/mol)	ΔH_{ele} (kJ/mol)	ΔS_{ele} (kJ/mol)	K
CO and H_2O passing into Cu-TiN	113740	-765660	-2950	-45907.93
CO and H_2O passing between Cu-TiN	1033320	1215390	610	-417068.65

H_2O are adsorbed on Cu in TiN-NT by weak bond (Figures 3 and 4). The electric resistance for them is following as:

$$E_{elec} = RI \qquad (4)$$

Where, E_{elec} is electric energy (V), R (Ω) is electric resistance and I (A) is electric intensity that is $I = \frac{q}{t}$ and q(C) is electric charge and t is time interaction, in experimental data, it is so:

Time (s)

Figure 7. The resistance (Ω), interaction CO and H_2O into Cu-TiN nanotube at 298K.

Time (s)
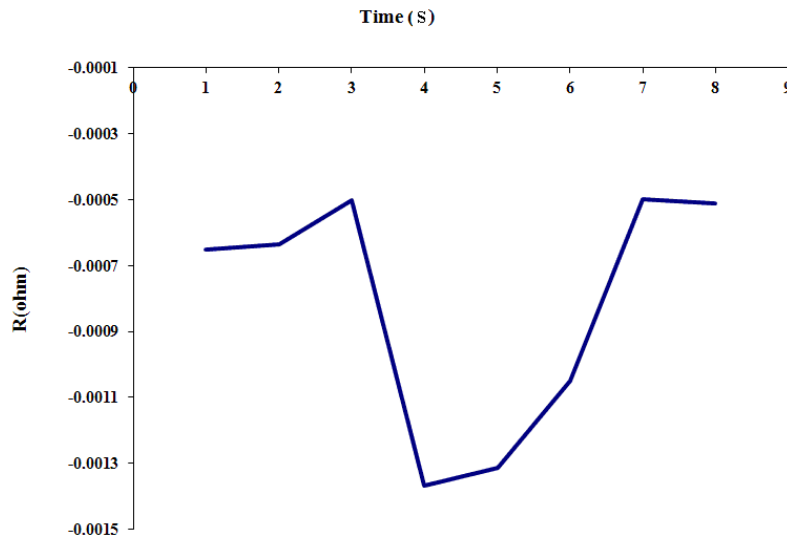
Figure 8. The resistance (Ω), interaction CO and H_2O between Cu-TiN nanotubes at 298K.

$$R = \frac{E_{elec} t}{nF} \qquad (5)$$

Where, n, F and t are electron number of conversion, faraday constant and time (h) respectively (Lee, 2005). After adsorption of CO and $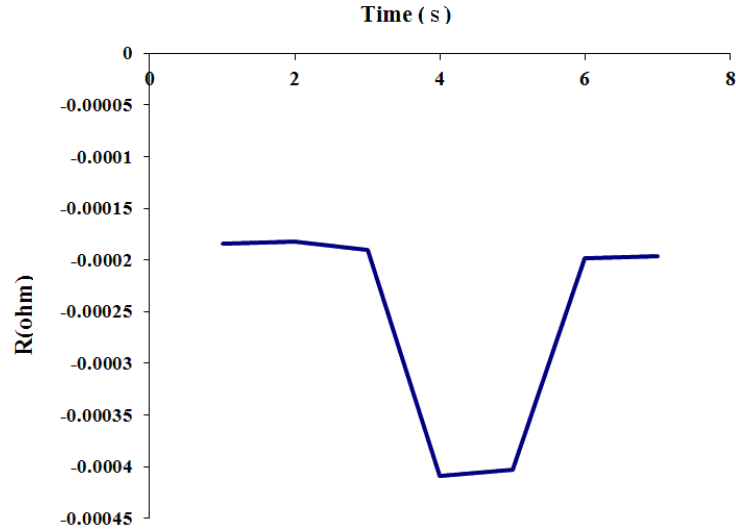H_2O$ on surface of Cu nanoparticles in TiN-NT and transition electron between them, the electric resistance to time (s) decreased that showed in Figures 7 and 8, when methanol is formed, the electric resistance is increasing.

TiN-nanotube is used as a photocatalyst in photocatalysis process, because is a semiconductor (Varghese et al., 2009). The absorption of a photon (hv) with ultra-band energy from UV irradiation source is caused TiN activation (Figure 9). The transmission of an electron (e^-) from the valence band to the conduction band is caused highly reactive positive holes (h^+) in the valence band, therefore this transfer is been to adsorption and conversion to pollutants on the Cu nanoparticles into low-risk products in environment:

$$TiN\text{-}NT + hv \rightarrow TiN\text{-}NT \ (e_{cb}^- + hole_{vb}^+)$$
$$H_2O \rightarrow OH^- + H^+$$
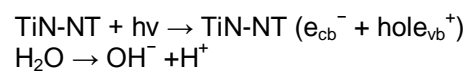
Figure 9. The electron transition from valance band (VB) to conduction band (CB) in semiconductor Cu-TiN-nanotube.

Oxidative reaction:

$$hole_{vb}^+ \; OH_{ads}^- \rightarrow \; ^\bullet OH$$
$$^\bullet OH + CO + HO_2 \rightarrow CH_3OH + O_2$$

Conclusion

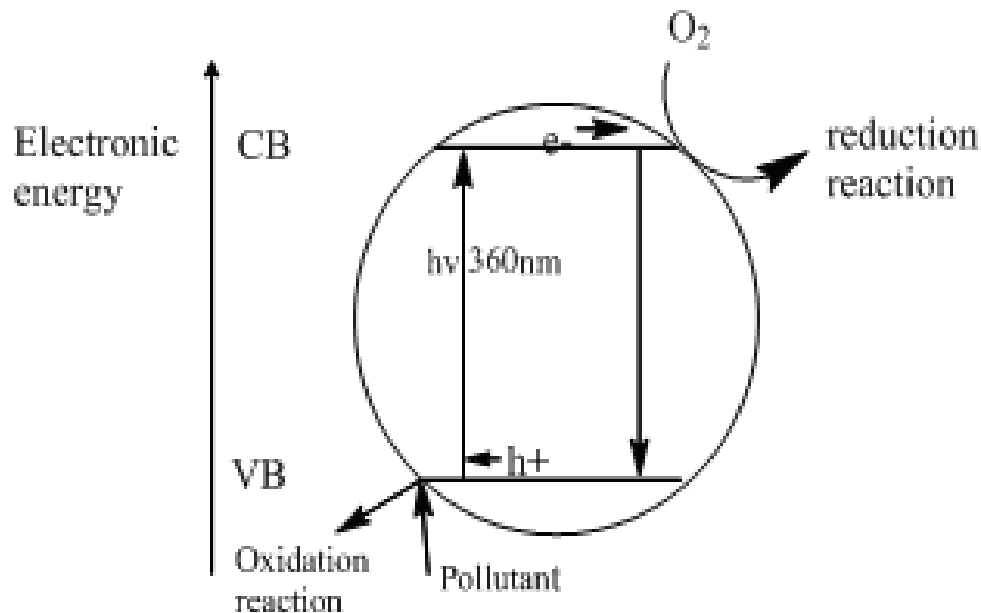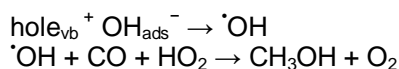After adsorption of CO onto the nanosurface and transference of electrons between them, the electric resistance decreased. The TiN-NTs are semiconductors, photo-active catalysts, able to utilize near-UV light, biologically, chemically inert, photo-stable and inexpensive, therefore TiN-NT is appropriate for this conversion in environment.

The co-catalysts of Cu and TiN with a nano structure significantly enhance the photocatalytic reduction of CO with H_2O to CH_3OH and O_2. In this manuscript this conversion to CH_3OH is calculated, the local minimum geometries of them were determined at B3LYP/6-31G level. The ZINDO/1 method is used for calculation of thermodynamic parameters these interactions. The calculation which shows heat reaction formation (ΔH) is endothermic for these reactions. These reactions need sun, photo active or other energy in presence of visible light. We propose, TiN nanotubes with Cu nanoparticles to form filter to be installed in exhaust of automobile and heat of exit gases provides energy to the converter. These techniques have been highly considered by researchers and industrial men because of their low cost, high adsorption efficiency, selective operation, easy and hazardless application.

Conflict of Interest

The authors have not declared any conflict of interest.

REFERENCES

Aresta M, Dibenedetto A (2004). The contribution of the utilization option to reducing the CO_2 atmospheric loading: research needed to overcome existing barriers for a full exploitation of the potential of the CO2 use. Catal. Today. 98:455–462. http://dx.doi.org/10.1016/j.cattod.2004.09.001

Becke D (1993). Densityfunctional thermochemistry. III. The role of exact exchange. J.Chem.Phys. 98:5648-5652. http://dx.doi.org/10.1063/1.464913

Dondela B, Peszke J, Śliwa W (2005). Semiempirical ZINDO/S, AM1 and ab initio HF/STO-3G and HF/6-31G study of quaternary salts of diazaphenanthrenes with ethyl bromide and 1,3-dibromopropane. J. Mol. Structure. 753(1–3):154–164. http://dx.doi.org/10.1016/j.molstruc.2005.06.016

Farha OK, Yazaydin O, Eryazici I, Malliakas C, Hauser B, Kanatzidis MG, Nguyen ST, Snurr RQ, Hupp JT (2010). De novo synthesis of a metal-organic framework material featuring ultrahigh surface area and gas storage capacities. Nat. Chem. 2:944–948. http://dx.doi.org/10.1038/nchem.834

Hohenberg P, Kohn W (1964). Inhomogeneous electron gas. Phys. Rev.136:B864-B871. http://dx.doi.org/10.1103/PhysRev.136.B864

Kolmakov A, Zhang Y, Cheng G, Moskovits M (2003). Detection of CO and O2 using Tin Oxide Nanowire Sensors. Adv. Mater. 15(12):997-1000. http://dx.doi.org/10.1002/adma.200304889

Lee S (2005). Encyclopedia of chemical processing and design. Taylor & Francis, 2005. ISBN: 0824755634, 9780824755638.

Li J, Zhao Z, Kazakov A, Chaos M, Dryer FL, Jr JJS (2007). A comprehensive kinetic mechanism for CO, CH2O, and CH3OH combustion. Int. J. Chemical Kinetics. 39(3):109–136. http://dx.doi.org/10.1002/kin.20218

Paulose M, Shankar K, Yoriya S, Prakasam HE, Varghese OK, Mor GK,

Latempa TA, Fitzgerald A, Grimes CA (2006). Anodic Growth of Highly Ordered TiO_2 Nanotube Arrays to 134 μm in Length. J. Phys. Chem. B 110(33):16179-16184. http://dx.doi.org/10.1021/jp064020k

Reslan R, Lopata K, Arntsen C, Govind N, Neuhauser D (2012). Electron transfer beyond the static picture: A TDDFT/TD-ZINDO study of a pentacene dimer. HE. J. Chem. Phys. 137:22A502-6. http://dx.doi.org/10.1063/1.4729047

Ridley J, Zerner M (1973). An intermediate neglect of differential overlap technique for spectroscopy: Pyrrole and the azines. Theoretica chimica acta. 32(2):111-134. http://dx.doi.org/10.1007/BF00528484

Riduan SN, Zhang Y, Ying JY (2009). Conversion of carbon dioxide into methanol with silanes over N-Heterocyclic Carbene Catalysts. Angew. Chem. 121:3372–3375. http://dx.doi.org/10.1002/ange.200806058

Varghese OK, Paulose M, LaTempa TJ, Grimes AG (2009). High-rate solar photocatalytic conversion of CO_2 and water vapor to hydrocarbon fuels. Nano. Lett. 9(2):731-737. http://dx.doi.org/10.1021/nl803258p

Yang DA, Cho HY, Kim J, Yang ST, Ahn WS (2012). CO_2 capture and conversion using Mg-MOF-74 prepared by a sonochemical method. Energy Environ. Sci. 5:6465–6473. http://dx.doi.org/10.1039/c1ee02234b

Yang LW, Parr RG (1988). Development of the colle-salvetti correlation-energy formula into a functional of the electron density Phys. Rev. B: Condens. Matter. 37:785-789. http://dx.doi.org/10.1103/PhysRevB.37.785

Zerner M (1991). Reviews in computational chemistry, Volume 2, Eds. K. B. Lipkowitz and D. B. Boyd, VCH, New York, P. 313. http://dx.doi.org/10.1002/9780470125793.ch8

Full Length Research Paper

Construction of some new exact structures for the nonlinear lattice equation

W. Djoudi and A. Zerarka*

Laboratory of Applied Mathematics, University Med Khider, BP145, 07000 Biskra; Algeria.

In the present work we examine a generalized coth and csch functions method to construct new exact travelling solutions to the nonlinear lattice equation. The technique of the homogeneous balance method is used to handle the appropriated solutions. Some exact solutions obtained are new.

Key words: Nonlinear lattice, travelling wave solutions.

INTRODUCTION

Several methods have been developed for analytic solving of nonlinear partial differential equations. Specially, almost all of these nonlinear model equations were appeared (Wang and Li, 2008; Korteweg and Vries, 1995; Khelil et al., 2006) to give different structures to the solutions. Besides traditional methods such as auto-Backlund transformation, Lie Groups, inverse scattering transformation and Miura's transformation, a vast variety of the direct methods for obtaining explicit travelling solitary wave solutions have been found (Zerarka and Foester, 2005; Ibrahim and El-Kalaawy, 2007; Lü, 2014a,b). The availability of symbolic computation packages can be facilitating many direct approaches to establish solutions to non-linear wave equations (Xu and Zhang, 2007; Özis and Yıldırım, 2008). Various extension forms of the sine-cosine and tanh methods proposed by Malfliet and Wazwaz have been applied to solve a large class of nonlinear equations (Malfliet 1996a,b; Wazwaz 2004; He and Wu, 2006a,b). More importantly, another mathematical treatment is established and used in the

analysis of these nonlinear problems, such as Jacobian elliptic function expansion method, the variational iteration method, pseudo spectral method, the averaging method, and many others powerful methods (Odibat and Momani, 2006; Rafei and Ganji, 2006; Yu, 2007; Zhu, 2007a,b; Lü and Peng, 2013a,b,c; Lü, 2013; Lü et al., 2010; Jia et al., 2014; Liu and Qian, 2011). The aim of this work is to propose an efficient approach to examine new developments in a direct manner without requiring any additional condition on the investigation of exact solutions with the coth and csch functions method for a lattice system. We expect that the presented method could lead to construct successfully many other solutions for a large variety of other nonlinear evolution equations.

ANALYSIS OF THE PROBLEM

We consider the following nonlinear problem for the lattice equation as:

$$R(u, u_t, u_x, u_y, u_z, u_{xy}, u_{yz}, u_{xz}, u_{xx}, ...) = 0, \qquad (1)$$

Here the subscripts represent partial derivatives, and $u(t, x, y, z, ...)$ is an unknown function to be determined. We take the following transformation for the new wave variable as:

$$\xi = \sum_{i=0}^{p} \alpha_i \chi_i + \delta, \qquad (2)$$

χ_i are distinct variables, and when $p = 1$, $\xi = \alpha_0 \chi_0 + \alpha_1 \chi_1 + \delta$, the quantities α_0, α_1 are called the wave pulsation ω and the wave number k respectively if χ_0, χ_1 are the variables t and x respectively. In the discrete case for the position x and with continuous variable for the time t, ξ becomes with some modifications $\xi_n = nd + ct + \delta$ and n is the discrete variable. d and δ are arbitrary constants and c is the velocity. We use the traveling wave reduction transformation for Equation (1) as:

$$u(\chi_0, \chi_1, ...) = U(\xi), \qquad (3)$$

and the chain rule

$$\frac{\partial}{\partial \chi_i}(.) = \alpha_i \frac{d}{d\xi}(.), \quad \frac{\partial^2}{\partial \chi_i \partial \chi_j}(.) = \alpha_i \alpha_j \frac{d^2}{d\xi^2}(.), \cdots, \qquad (4)$$

Upon using Equations (3) and (4), the nonlinear problem (1) becomes an ODE like

$$Q(U, U_\xi, U_{\xi\xi}, U_{\xi\xi\xi}, U_{\xi\xi\xi\xi}, ...) = 0 \qquad (5)$$

APPLICATIONS

The one-dimensional lattice equation (Zhu, 2007, 2008) is written as:

$$\frac{du(n,t)}{dt} - (a + bu(n,t) + u^2(n,t))[u(n+1,t) - u(n-1,t)] = 0, \qquad (6)$$

We first combine the independent variables, into a wave variable using ξ_n as

$$\xi_n = nd + ct + \delta \qquad (7)$$

and we take the travelling wave solutions of the system

(6) using Equation (7) as $u(n,t) = U(\xi_n)$. By using the chain rule (4), the system (6) can be obtained as follows:

$$cU_{\xi_n}(\xi_n) - (a + bU(\xi_n) + U^2(\xi_n))(U(\xi_{n+1}) - U(\xi_{n-1})) = 0, \qquad (8)$$

Where subscript denotes the differential with respect to ξ_n.

THE COTH FUNCTION METHOD

Suppose that Equation (8) has the following solution:

$$U(\xi_n) = \sum_{j=0}^{M} A_j \coth^j(\xi_n), \qquad (9)$$

Where M is an undetermined integer and A_j are coefficients to be determined later. In order to determine values of the parameter M, we balance the linear term of highest order in Equation (8) with the highest order nonlinear term. By simple calculation, we have $2M = M + 1$ and the solution (9) takes the form

$$U(\xi_n) = A_0 + A_1 \coth(\xi_n), \qquad (10)$$

Substituting the solution (10) into Equation (8), and equating to zero the coefficients of all powers of $\coth^j(\xi_n)$ yields a set of algebraic equations for A_0, A_1 and c as:

$$bA_1 + 2A_0 A_1 = 0$$
$$2(a + bA_0 + A_0^2) = c \coth(d) \qquad (11)$$
$$-2A_1^2 \coth(d) = c$$

Solving the system of algebraic equations with the aid of Mathematical, we obtain

$$A_0 = -\frac{b}{2},$$
$$A_1 = \pm \frac{\tanh(d)}{2} \sqrt{b^2 - 4a}, \qquad (12)$$
$$c = \frac{\tanh(d)}{2}(4a - b^2),$$

and the two travelling wave solutions of the problem of interest follow

$$U_\pm(\xi_n) = -\frac{b}{2} \pm \frac{\tanh(d)}{2} \sqrt{b^2 - 4a} \coth\left[nd + \frac{\tanh(d)}{2}(4a - b^2)t + \delta\right] \qquad (13)$$
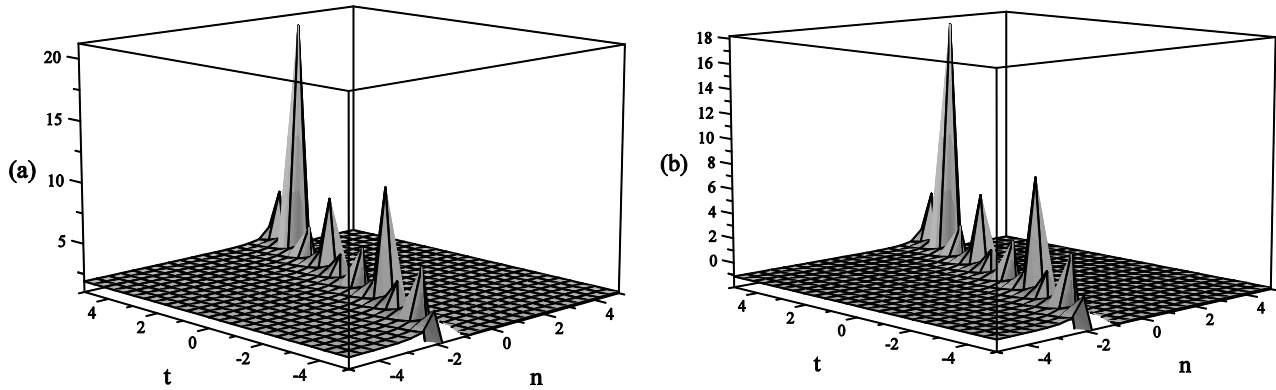
Figure 1. The graphs show the wave solutions of $u_{\pm}(n,t) = U_{\pm}(\xi_n)$ in Equation (13): (a) solution $u_+(n,t) = U_+(\xi_n)$, (b) solution $u_-(n,t) = U_-(\xi_n)$. For both curves: $a = 2, b = 3, d = 1, \delta = 0$.

Where d and δ are arbitrary constants.

Figure 1(a) and (b) show the physical waves $u_+(n,t) = U_+(\xi_n)$ and $u_-(n,t) = U_-(\xi_n)$ in Equations (13).

THE COTH-CSCH FUNCTION METHOD

The solutions of Equation (8) can be expressed in the form

$$U(\xi_n) = \alpha + \sum_{j=1}^{M} A_j \coth^j(\xi_n) + B_j \operatorname{csch}^j(\xi_n), \qquad (14)$$

Where α, A_j and B_j are parameters to be determined.

The parameter M is found by balancing the highest-order linear term with the nonlinear terms, we obtain $M = 1$, and $U(\xi_n)$ becomes

$$U(\xi_n) = \alpha + A \coth(\xi_n) + B \operatorname{csch}(\xi_n), \qquad (15)$$

Substituting Equation (15) into the relevant nonlinear differential Equation (8) and with the help of Mathematical we get a system of algebraic equations with respect to c, α, A and B.

$$Ac + 2A(A^2 + B^2)\coth(d) + 4AB^2 \operatorname{csch}(d) = 0,$$
$$4A^2 B \coth(d) + Bc \coth(d)^2 - 2B(\alpha^2 - B^2 + a + \alpha b)\operatorname{csch}(d) = 0,$$
$$-(Bc) - 4A^2 B \coth(d) - 2B(A^2 + B^2)\operatorname{csch}(d) = 0,$$
$$2A(2\alpha B + Bb) = 0,$$
$$2A(2A\alpha + Ab)\coth(d) + 2B(2\alpha B + Bb)\operatorname{csch}(d) = 0,$$
$$2A(\alpha^2 - B^2 + a + \alpha b) - Ac \coth(d) = 0 \quad (16)$$

After some algebra, and with the help of Mathematical, the following values for the parameters c, α, A, and B are obtained:

First set

$$c = \frac{1}{2}(4a - b^2)\tanh(d),$$

$$\alpha = -\frac{b}{2}, \qquad (17)$$

$$A = \pm\frac{1}{2}\sqrt{b^2 - 4a}\,\tanh(d),$$

$$B = 0,$$

and the travelling solutions of Equation (17) are obtained as:

$$U_{\pm}(\xi_n) = -\frac{b}{2} \pm \frac{\tanh(d)}{2}\sqrt{b^2 - 4a}\,\coth(\xi_n), \qquad (18)$$

Where $\xi_n = nd + \frac{\tanh(d)}{2}(4a - b^2)t + \delta$. The solutions (18) are similar to those obtained by the coth-function method Equation (13).

Second set

$$c = \frac{1}{2}(4a - b^2)\sinh(d),$$

$$\alpha = -\frac{b}{2}, \qquad (19)$$

$$A = 0,$$

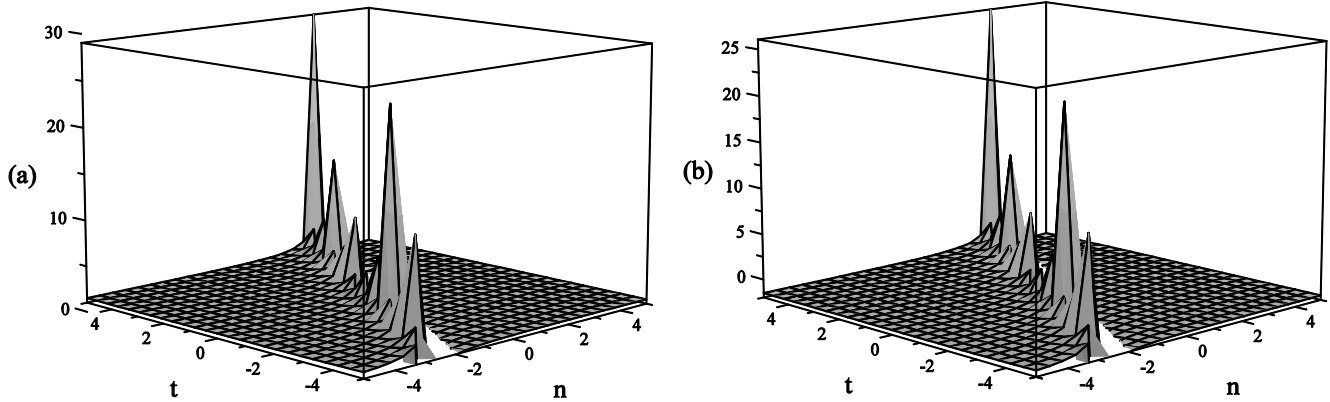$$B = \pm\frac{1}{2}\sqrt{b^2 - 4a}\,\sinh(d),$$

Figure 2. The graphs show the wave solution of $U_\pm(\xi_n)$ in (20): (a) solution $u_+(n,t) = U_+(\xi_n)$, (b) solution $u_-(n,t) = U_-(\xi_n)$. For both curves: $a = 2, b = 3, d = 1, \delta = 0$.

and the travelling solutions of Equation (19) are obtained as

$$U_\pm(\xi_n) = -\frac{b}{2} \pm \frac{\sinh(d)}{2}\sqrt{b^2 - 4a}\, \mathrm{csch}(\xi_n), \qquad (20)$$

Where $\xi_n = nd + \frac{\sinh(d)}{2}(4a - b^2)t + \delta$. The portraits of solutions (20) for $U_\pm(\xi_n)$ are displayed in Figure 2(a) and (b).

Third set

$$
\begin{aligned}
c &= \left(4a - b^2\right)\tanh\left(\frac{d}{2}\right), \\
\alpha &= -\frac{b}{2}, \\
A &= \pm\frac{1}{2}\sqrt{b^2 - 4a}\,\tanh\left(\frac{d}{2}\right), \\
B &= \pm\frac{1}{2}\sqrt{b^2 - 4a}\,\tanh\left(\frac{d}{2}\right),
\end{aligned}
\qquad (21)
$$

Finally, third set admits the following two types:

$$U_{1\pm}(\xi_n) = -\frac{b}{2} - \frac{1}{2}\tanh\left(\frac{d}{2}\right)\sqrt{b^2 - 4a}\,(\coth(\xi_n) \pm \mathrm{csch}(\xi_n)), \qquad (22)$$

and

$$U_{2\pm}(\xi_n) = -\frac{b}{2} + \frac{1}{2}\tanh\left(\frac{d}{2}\right)\sqrt{b^2 - 4a}\,(\coth(\xi_n) \pm \mathrm{csch}(\xi_n)), \qquad (23)$$

Where $\xi_n = nd + \left(4a - b^2\right)\tanh(\frac{d}{2})t + \delta$. The behaviors of solutions (22) and (23) for $U_{1+}(\xi_n)$ and $U_{2+}(\xi_n)$ are shown in Figure 3(a) and (b) respectively. The solutions given for the second and the third sets appear to be new.

CONCLUSION

The basic goal of this work, is to provide a new trial travelling solution to build the exact solutions to the nonlinear lattice equation. Two types of functions are used to find the exact solutions, which are named the coth-function and the coth-csch function methods. Eight variants of travelling wave solutions are obtained. The present method provides a reliable technique that requires less work if compared with the difficulties arising from computational aspect. The main advantage of this method is the flexibility to give exact solutions to nonlinear problems without linearization. We may conclude that, this method can also be extended to other high-dimensional nonlinear phenomena. It will be then interesting to study more general systems. These points will be investigated in a future research.

Conflict of Interest
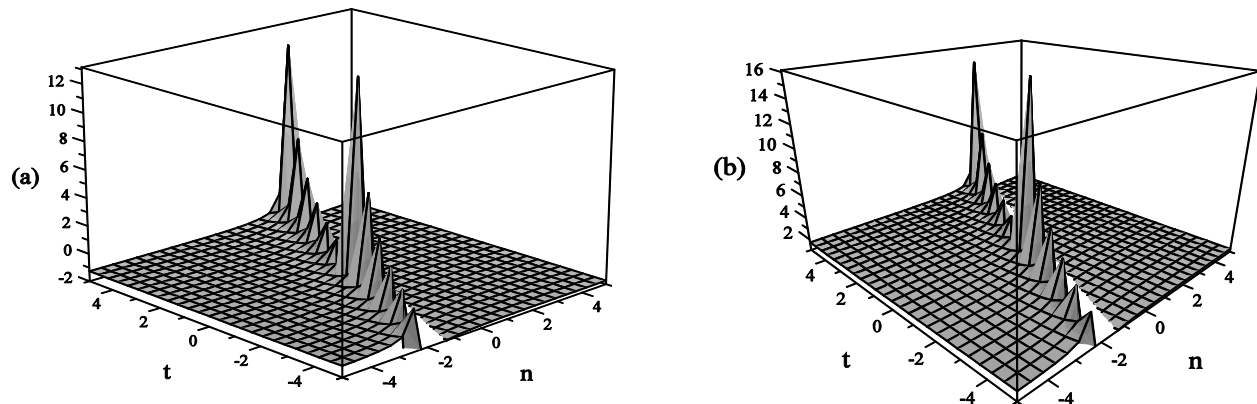
The authors have not declared any conflict of interest.

Figure 3. The graphs show the wave solution of $U_{1\pm}(\xi_n)$ and $U_{2\pm}(\xi_n)$ in (22) and (23) respectively: (a) solution $u_{1+}(n,t) = U_{1+}(\xi_n)$, (b) solution $u_{2+}(n,t) = U_{2+}(\xi_n)$. For both curves: $a = 2, b = 3, d = 1, \delta = 0$.

REFERENCES

He JH, Wu XH (2006a). Exp-function method for nonlinear wave equations. Chaos Solitons Fractals. 30(3):700-708. http://dx.doi.org/10.1016/j.chaos.2006.03.020

He JH, Wu XH (2006b). Construction of solitary solution and compacton-like solution by variational iteration method. Chaos Solitons Fractals. 29(1):108-113. http://dx.doi.org/10.1016/j.chaos.2005.10.100

Ibrahim RS, El-Kalaawy OH (2007). Extended tanh-function method and reduction of nonlinear Schrödinger-type equations to a quadrature. Chaos Solitons Fractals. 31(4):1001-1008. http://dx.doi.org/10.1016/j.chaos.2005.10.055

Jia L, Liu Q, Ma Z (2014). A good approximation of modulated amplitude waves in Bose–Einstein condensates. Communications in Nonlinear Sci. Numer. Simul. 19(8):2715-2723. http://dx.doi.org/10.1016/j.cnsns.2013.12.034

Khelil N, Bensalah N, Saidi H, Zerarka A (2006). Artificial perturbation for solving the Korteweg-de Vries equation. J. Zhejiang Univ. SCI. A 7(12):2079-2082.

Korteweg DJ, de Vries G (1995). On the change of the form of long waves advancing in a rectangular canal and on a new type of long stationary waves. Philos. Mag. P. 39.

Liu Q, Qian D (2011). Modulated amplitude waves with nonzero phases in Bose-Einstein condensates. J. Math. Phys. 52(8):082702. http://dx.doi.org/10.1063/1.3623415

Lü X (2014a). New bilinear Backlund transformation with multisoliton solutions for the (2+1)-dimensional Sawada-Kotera model. Nonlinear Dyn. 76:161. http://dx.doi.org/10.1007/s11071-013-1118-y

Lü X (2014b), Bright-soliton collisions with shape change by intensity redistribution for the coupled Sasa-Satsuma system in the optical fiber communications, Communications in Nonlinear Science and Numerical Simulation, 19:3969. http://dx.doi.org/10.1016/j.cnsns.2014.03.013

Lü X, Peng M (2013a). Nonautonomous motion study on accelerated and decelerated solitons for the variable-coefficient Lenells-Fokas model. Chaos. 23:013122. http://dx.doi.org/10.1063/1.4790827

Lü X, Peng M (2013b). Systematic construction of infinitely many conservation laws for certain nonlinear evolution equations in mathematical physics. Commun. Nonlinear Sci. Numer. Simulat. 18:2304. http://dx.doi.org/10.1016/j.cnsns.2012.11.006

Lü X, Peng M (2013c). Painleve-integrability and explicit solutions of the general two-coupled nonlinear Schrodinger system in the optical fiber communications. Nonlinear Dyn. 73:405. http://dx.doi.org/10.1007/s11071-013-0795-x

Lü X (2013). Soliton behavior for a generalized mixed nonlinear Schrodinger model with N-fold Darboux transformation. Chaos. 23:033137. http://dx.doi.org/10.1063/1.4821132

Lü X, Tian B, Zhang HQ, Xu T, Li H (2010). Integrability study on the generalized (2+1)-dimensional variable-coefficient Gardner model with symbolic computation. Chaos. 20:043125. http://dx.doi.org/10.1063/1.3494154

Malfliet W (1996a). The tanh method: I. Exact solutions of nonlinear evolution and wave equations. Phys. Scr. 54:563-568. http://dx.doi.org/10.1088/0031-8949/54/6/003

Malfliet W (1996b). The tanh method:II.Perturbation technique for conservative systems. Phys. Scr. 54:569-575. http://dx.doi.org/10.1088/0031-8949/54/6/004

Odibat ZM, Momani S (2006). Application of variational iteration method to nonlinear differential equations of fractional order. Int. J. Nonlinear Sci. Numer. Simul. 7(1):27-34. http://dx.doi.org/10.1515/IJNSNS.2006.7.1.27

Özis T, Yıldırım A (2008). Reliable analysis for obtaining exact soliton solutions of nonlinear Schrödinger (NLS) equation. Chaos Solitons Fractals. 38:209-212. http://dx.doi.org/10.1016/j.chaos.2006.11.006

Rafei M, Ganji DD (2006). Explicit solutions of Helmholtz equation and fifth-order KdV equation using homotopy perturbation method. Int. J. Nonlinear Sci. Numer. Simul. 7(3):321-328. http://dx.doi.org/10.1515/IJNSNS.2006.7.3.321

Wang DS, Li H (2008). Symbolic computation and non-travelling wave solutions of (2+1)-dimensional nonlinear evolution equations. Chaos Solitons Fractals. 38:383-390. http://dx.doi.org/10.1016/j.chaos.2007.07.062

Wazwaz AM (2004). The tanh method for travelling wave solutions of nonlinear equations. Appl. Math. Comput. 154(3):713-23. http://dx.doi.org/10.1016/S0096-3003(03)00745-8

Xu LP, Zhang JL (2007). Exact solutions to two higher order nonlinear Schrödinger equations. Chaos Solitons Fractals. 31:937-942. http://dx.doi.org/10.1016/j.chaos.2005.10.063

Yu YX (2007). Rational formal solutions of hybrid lattice equation. Appl. Math. Comput. 186:474-482. http://dx.doi.org/10.1016/j.amc.2006.07.112

Zerarka A, Foester VG (2005). Separation method for solving the generalized Korteweg --de Vries equation. Comm. Nonlinear. Sci. Numer. Simul. 10:217-225. http://dx.doi.org/10.1016/j.cnsns.2003.09.003

Zhu SD (2007a). Exp-function method for the hybrid-lattice systems. Int. J. Nonlinear Sci. Numer. Simul. 8:461-464. http://dx.doi.org/10.1515/IJNSNS.2007.8.3.465

Zhu SD (2007b). Exp-function method for the discrete mkdv lattice. Int. J. Nonlinear Sci. Numer. Simul. 8:465-468. http://dx.doi.org/10.1515/IJNSNS.2007.8.3.461

Zhu SD (2008). Discrete (2+1)-dimensional toda lattice equation via exp-function method. Phys. Lett. A 372(5):654-657. http://dx.doi.org/10.1016/j.physleta.2007.07.085

International Journal of Physical Sciences

Science

Related Journals Published by Academic Journals

■African Journal of Pure and Applied Chemistry
■Journal of Internet and Information Systems
■Journal of Geology and Mining Research
■Journal of Oceanography and Marine Science
■Journal of Environmental Chemistry and Ecotoxicology
■Journal of Petroleum Technology and Alternative Fuels